Sodium butyrate alleviates chronic alcoholic neuroinflammation by regulating microgila polarization through GPR109A / PPAR-γ / NF-κB signaling pathway

Huiling Wei
School of Basic Medical Sciences, Ningxia Medical University, Yinchuan 750004, Ningxia
Yi Ren
Clinical Medical College, Ningxia Medical University, Yinchuan 750004, Ningxia
Chunyang Yu
School of Basic Medical Sciences, Ningxia Medical University, Yinchuan 750004, Ningxia
Chun Zhang
Ningxia Key Laboratory of Cerebrocranial Diseases, Ningxia Medical University, Yinchuan 750004, Ningxia
Li Guo
School of Basic Medical Sciences, Ningxia Medical University, Yinchuan 750004, Ningxia
Ting Wang
School of Basic Medical Sciences, Ningxia Medical University, Yinchuan 750004, Ningxia
Feifei Chen
School of Basic Medical Sciences, Ningxia Medical University, Yinchuan 750004, Ningxia
Xiaoxia Zhang
College of Traditional Chinese Medicine, Ningxia Medical University, Yinchuan 750004, Ningxia
Hao Wang
School of Basic Medical Sciences, Ningxia Medical University, Yinchuan 750004, Ningxia
Juan Liu (ryuken0518@163.com)
School of Basic Medical Sciences, Ningxia Medical University, Yinchuan 750004, Ningxia

Case Report

Keywords: Sodium butyrate, Alcohol, Microglia, Neuroinflammation, Cognitive dysfunction, GPR109A

Posted Date: June 22nd, 2022

DOI: https://doi.org/10.21203/rs.3.rs-1759989/v1

Abstract

Background

Alcohol can cause neuroinflammation, leading to neuron damage and further memory and cognitive impairment. Recent animal studies have shown that the exposure to chronic alcohol consumption induces robust inflammatory microglial activation in the brain. However, as a novel anti-inflammation approach, the impact of sodium butyrate on chronic alcohol-induced neuroinflammation still remains unclear.

Methods

Sixty female C57BL/6J mice were randomly divided into 4 groups: pair-fed (PF) group (PF/CON), alcohol-fed (AF) group (AF/CON), PF with sodium butyrate (NaB) group (PF/NaB) and AF with NaB group (AF/NaB). Each group was fed a modified Lieber-DeCarli liquid diet with or without alcohol. Mice were subjected to different behavioral tests to assess aberrant behaviours (deficits in cognitive functions, depression and anxiety). Pathological changes were further investigated by Hematoxylin and eosin staining (HE) and Nissl staining. The microglial activation and microglial polarization were observed by immunohistochemistry (IHC), immunofluorescence (IF) and flow cytometry. Enzyme-linked immunosorbent assay (ELISA) was used to determine the levels of inflammatory factors. G-protein coupled receptor 109A (GPR109A), peroxisome proliferator-activated receptor γ (PPAR-γ) and nuclear factor-κB (NF-κB) mRNA and protein levels were evaluated by reverse transcription-quantitative (RT-q) PCR and western blot (WB).

Results

As indicated by the behavioural tests, inflammatory indicators, microglial activation (M1/M2 microglia polarization) and brain morphology, sodium butyrate administration ameliorated aberrant behaviours (locomotor hypoactivity, anxiety disorders and depressive behaviours, impaired learning and spatial recognition memory), effectively reduced neuroinflammation and neuronal damage. The effectiveness of sodium butyrate may attribute to the GPR109A receptor in microglia by up-regulating the expression of PPAR-γ and inhibiting the activation of NF-κB.

Conclusion

Sodium butyrate ameliorates neuroinflammation induced by chronic alcohol exposure and improves memory and cognitive functions in mice via modulating microglia-mediated GPR109A / PPAR-γ / NF-κB signaling pathway.

1. Introduction

The World Health Organization (WHO) estimates that 2.3 billion people consume alcohol worldwide and 75 million suffer to alcohol disorders which trigger multi- systemic injuries predominantly in liver, gut, and brain[1]

In the central nervous system (CNS), chronic alcohol consumption results in cognitive deficiency, motor deficits, behaviors associated with anxiety[2–4]. Some researchers have demonstrated that chronic alcohol ingestion can lead to hippocampal inflammation in the brain, causing morphologically and functionally abnormal hippocampal neurons and synapses[5]. The hippocampus is a crucial brain structure for learning and memory, and its damage leads to the progression of severe cognitive impairments[6]. In addition to alcoholic liver disease (ALD), alcohol-related neuroinflammation and cognitive dysfunction can give rise to disability, even death, which brings heavy burden to society and family. Therefore, effective drug therapies for neuroinflammatory cognitive impairment induced drug abuse are limited and urgently needed.

Alcohol is a psychoactive substance with several neurobiological effects that can cause both acute and chronic injury in the brain, including neuroinflammation and neurodegeneration[7]. Further, microglia, a resident macrophage of the CNS, can be activated in the brain after excessive alcohol intake[8]. An increasing number of studies show that microglial activation contributes to the neuroinflammation correlated with chronic alcohol exposure[9]. Activation of microglias and inflammatory phenotypes are critical for the neuroprotection, but persistent abnormal activation of microglias and associated neuroinflammatory responses are one of the core pathological features of neurodegenerative diseases[10]. With regard to their activation, microglia are commonly polarized into M1 (pro-inflammatory) and M2 (anti-inflammatory)[11, 12]. M1 microglia secretes pro-inflammatory mediators such as tumor necrosis factor-α (TNF-α), interlukin-1β (IL-1β), interlukin-6 (IL-6), and nitric oxide synthase (iNOS). Due to the sources of neurotoxins, chronically activated M1 microglia influences the viability and function of neurons and are thought to exacerbate neuronal injury. In contrast, M2 microglia with the generation of anti-inflammatory mediators such as arginase-1 (Arg1) and anti-inflammatory interleukin-10 (IL-10) plays an important role in neuronal development and neuroprotection[13]. Imbalance of M1/M2 polarization or re-polarization of resident microglia is usually associated with inflammation, infection and autoimmune disorders[14]. Thus, the understanding of microglia in neuroinflammation after chronic alcohol exposure may be the key to improve cognitive dysfunction.

Butyrate, one of the short chain fatty acids (SCFAs), is naturally produced by symbiotic bacteria in the gastrointestinal tract through fermenting dietary fibers. Numerous studies have proved that sodium butyrate is a preferred energy source for colon epithelial cells, contributing to the maintenance of the gut barrier and immunological modulation[15]. Immunomodulatory effects of butyrate were studied in a wide range of intestinal diseases, of which the mechanism suggested was through the modulation of TNF-α-induced nuclear factor-κB (NF-κB) and peroxisome proliferator-activated receptor-γ (PPAR-γ)[16–18]. M1 polarization involves the activation of NF-κB, while M2 polarization is driven by PPAR-γ stimulation[19].

Reportedly, PPAR-γ, a member of nuclear receptors, can directly combine with p65/p50 to reduce inflammatory DNA-binding activity of NF-κB[20]. Moreover, our own previous research has shown that during the amelioration of ALD, metabolic SCFAs mainly including butyric acid were improved and notably repressed the inflammation by regulating liver macrophage polarization[21, 22]. However, the exact impact of sodium butyrate on microglia in neuroinflammation after chronic alcohol exposure still remains unclear.

SCFAs have been described to activate 3 G-protein coupled receptors (GPRs): free fatty acid receptors 2 and 3 [FFA2 and 3, also referred to as GPR43 and GPR41], and niacin/butyrate receptor GPR109A, where acetate and propionate activate GPR-43 and − 41 while butyrate is the ligand for GPR109A[23]. Recent studies have shown that GPR109A is mainly expressed on immune cells (including dendritic cells, monocytes, macrophages and neutrophils) involved in an anti-inflammatory effect[24]. The activation of GPR109A can inhibit the production of pro-inflammatory cytokines in macrophages, low-density lipoprotein (LDL) uptake and chemotaxis[25]. In addition, GPR109A receptor has also been reported to be highly expressed in microglia[26].

Thus, this study aimed to investigate the impacts of sodium butyrate on alcohol exposure neuroinflammation and cognitive function, as well as the underlying regulation of microglia, which may potentially contribute to the control of chronic alcoholic neuroinflammatory injury.

2. Materials And Methods

2.1 Animals and Diets

Six-week-old female C57BL/6J mice, obtained from Animal experiment center of Ningxia Medical University and were placed in a polycarbonate cage with a temperature control chamber (ambient temperature 22 ± 2 ℃, air humidity 40%-70%), 12 h dark/light cycle in Animal Experiment Center of Ningxia Medical University. Lieber-DeCarli liquid feed including alcohol feed (product number: TP4030M3) and non-alcoholic feed (product number:TP4030M3C) were purchased from TROPHIC Animal Feed High-tech Co., LTD., Nantong, China. Sodium butyrate was obtained from Shanghai Beinuo Biotechnology Co., LTD (V900464-25G).

2.2 Experimental Design

After a 1-week period of acclimation of the control liquid diet, female C57BL/6J mice (n = 60, 6 weeks old) were fed the modified Lieber-DeCarli liquid diets as previously described[27]. Briefly, mice were randomly allocated into 4 groups (15 mice/group): (a) pair-fed (PF) group (PF/CON), mice were fed ethanol (EtOH)-free modified Lieber-DeCarli liquid diets as PF control (CON); (b) alcohol-fed (AF) group (AF/CON), mice were fed EtOH-containing modified Lieber-DeCarli liquid diets as AF control; (c) PF with sodium butyrate (NaB) group (PF/NaB), mice were fed EtOH-free modified Lieber-DeCarli liquid diets containing sodium butyrate as sodium butyrate control; and (d) AF with sodium butyrate group (AF/ NaB), mice were fed EtOH-containing modified LieberDeCarli liquid diets with sodium butyrate as sodium butyrate intervention

group. Mice in AF groups were fed the modified Lieber-DeCarli liquid diets containing EtOH with an energy composition of 18% protein, 19% carbohydrate, 35% fat, and 28% EtOH, whereas mice in PF groups (PF/CON and PF/NaB) received an equal amount of calories as AF groups with the alcohol-derived calories substituted with isocaloric maltose–dextrin (carbohydrate). Components of the liquid diets were shown in **Table S1**. Groups (a) and (c) were the pair-fed controls for groups (b) and (d), respectively. Liquid diets were freshly prepared from powder daily according to the manufacturer's instruction. Average daily volume of liquid intake per mouse was monitored and calculated in AF groups. Mice in PF groups consume equal amounts of diets. During the study, body weight was recorded weekly. After 6 weeks of feeding, mice were sacrificed and the associated indicators were investigated.

2.3 Behavioral analysis

2.3.1 New object recognition (NOR)

NOR experiments were used to evaluate the ability of mice to recognize new objects in the environment. First, mice were habituated in an empty white chamber box for 5 min. After 10 min, each mouse was returned to the same chamber with two identical objects placed in the corners and allowed to freely explore for 5 min. The time spent exploring each object was recorded. Exploration was defined as reaching the object, sniffing it from a distance of < 2 cm, and/or touching it with the nose. After 5 min, one object was replaced with a novel one, the mice were allowed to explore for another 5 min. The time spent by the mice exploring the novel and old objects was recorded and was used to calculate a recognition index as follows: (time novel) / (time novel + time old).

2.3.2 Morris water maze (MWM)

Spatial learning and memory were analyzed using the MWM task. The MWM was divided into four equal quadrants, and a platform was hidden 1 cm below the surface of the water. One day before starting training, for acclimation, the animals were made to swim freely in the swimming pool for 60 s without an escape platform. The training session consisted of 6 days, four trials per day, and the time spent for finding the hidden escape platform was recorded as escape latency for each mouse. If mice could not find the escape platform within 60 s, they were directed to land on the platform and allowed them to stay for 20 s. To test how well the animals had learned the position of the escape platform, we gave a probe trial at the end of training day 6 and mice were allowed to swim freely for 60 s with no escape platform. Video tracking was used to automatically measure how well the mice remembered the previous location of the escape platform.

2.3.3 Y- maze

Y-maze apparatus was used to assess spatial working memory. Y-maze consists of three long, wide, and high arms of 34, 10, and 10 cm, which are the starting arm, novel arm, and known arm, respectively. The experimental animals were placed in the test room to adapt to the environment 10 min before the experiment. During the first stage, the novel arm was blocked by a white baffle, allowing mice to only move freely in the other two arms for 5 min, and the mouse movement track and time were recorded in

the starting arm and known arms. Then the mice were placed in the starting arm, the novel arm was opened, the exploration was performed for 5 min, and the mouse movement track and time were still recorded. Memory performance was given by the percentage of time spent in the novel arm over the time spent exploring all arms.

2.3.4 Shuttle Box

Shuttle box, consisted of two equal-sized compartments with divided with a central inverted U-shaped gate, was used to evaluate the learning and memory ability of rodents. Each testing session began with acclimatization to the chambers for 2 min, followed by 30 trails with an inter-trial interval of 30 s. A tone (60 dB) and light (8 W) were co-administered as conditioned stimuli for 10 s in each assay. An electrical foot shock (0.3 mA) was used as the unconditioned stimulus and administered for 5 s following the presentation of the conditioned stimuli. The procedure was performed for a total of 5 days and the active evasions were monitored continuously.

2.3.5 Open field test (OFT)

The OFT was performed to evaluate anxiety and locomotor activity in mice. Mice were moved into the behavioral test room at least 1 h before the experiment. The test consisted of 10 min trial in a white opaque 40, 40, and 30 cm arena and the center zone defined as a square covering 25% of the total area and allowed to explore it freely for 10 min. Their ambulatory and rearing activities over the last 5 min were recorded using an automatic video tracking system (Smart version 3.0; Panlab, S.L.U., Barcelona, Spain). Moreover, the area was cleaned with 75% ethanol and allowed to dry completely between each test. The total travelled distance was considered as an index of locomotor activity. Rearing and defecation were considered indices for ‘anxiety levels’, while increased proportion of distance or time spent in the center indicated decreased anxiety.

2.3.6 Forced swim test (FST)

The FST was used to assess depressive behavior in rodents. Briefly, mice were placed into plastic buckets with 19 cm in diameter and 23 cm deep, filled with water at 25°C. The duration of mobility and immobility phases was recorded using an automatic video tracking system (Smart version 3.0; Panlab, S.L.U., Barcelona, Spain) within 5 min.

2.4 Hematoxylin and eosin staining (HE staining)

After the mice were anaesthetized, they were perfused intracardially with PBS and then fixed with 4% paraformaldehyde. Then, the brain and liver were extracted and fixed in 4% formaldehyde solution again for 24 h, washed with running water, dehydrated in ethanol, and paraffin-embedded, then sliced (5 μm thickness) and placed onto glass slides. HE staining of the brain tissues was conducted according to standard protocols. Briefly, after deparaffinization with xylene and rehydration with graded alcohol solutions, tissue sections were stained with hematoxylin solution (ZSGB-BIO, China) for 10–15 min followed by 2 dips in 1% acid ethanol (1% HCl in 75% ethanol) and rinsed in distilled water for 5 min. Then the sections were stained with eosin solution (ZSGB-BIO, China) for 3 min and rinsed again in

distilled water for 3 min. Ultimately, dehydration with graded alcohol solutions and clearing with xylene, the slides were sealed by neutral balata. The mounted and dried slides were then examined and photographed using an Olympus microscope (Aomori Olympus, BX51, Japan).

2.5 Nissl staining

Nissl staining was performed to analyze the degree of morphological changes in chronic alcohol exposed group and chronic alcohol exposed plus sodium butyrate -treated group. Sections (5 μm) were cut from each block on coated slides and dried overnight at 37°C. After that, tissue sections were deparaffinized with xylene followed by graded rehydration in ethanol (100%, 95%, 80%, and 70%) and distilled water. Then, sections were stained for 1h in the 0.5% cresyl violet solution (Nissl staining kit, Solarbio Technology, Beijing) at 60°C and washed with distilled water. Next, hydrochloric acid and ethanol were used for differentiation. The differentiation was controlled under endoscopy and terminated when the background was clean and Nissl bodies were clearly visible. Finally, the sections were dehydrated, cleared in xylene, and used neutral resin to seal the slices. The morphological changes of neurons in various hippocampal regions (CA1, CA3, and DG) and prefrontal cortex areas were observed under a microscope (Bar = 20 μm).

2.6 Immunohistochemistry staining (IHC staining)

IHC staining was performed using 5 μm paraffin-embedded brain tissue sections. The slides were dewaxed and rehydrated. Subsequently, the slides were washed 3 times with PBS, antigen retrieval was performed with sodium citrate in microwave oven at 100°C for 17 min, blocked in 20% normal goat serum, and incubated with rabbit antibody against Iba1 (1:8000; ab178847, Abcam, MA, USA) at 4°C overnight in a humidified container. After washes with PBS, the slides were incubated with horseradish peroxidase (HRP) -conjugated goat anti-rabbit immunoglobulin-G (IgG) secondary antibody (1:1000 dilution, Abbkine, No. A21020, China) for 30 min at 37°C. After 4 min of reaction with substrate-chromogen 3, 3'-diaminobenzidine, the slides were counterstained with hematoxylin after the IHC protocol. Images were captured with a microscope. Positive areas in 40 × optical fields of the prefrontal cortex, hippocampal DG, CA1, and CA3 regions. Quantification was done using Image J software.

2.7 Immunofluorescence staining (IF staining)

IF staining was performed at room temperature. In brief, mice were euthanized and perfused with PBS (0.01 M, pH 7.40, 4°C) transcardially first and then perfused with 4% paraformaldehyde (PFA) solution (pH 7.40, 4°C). The cerebrums were dissected before soaked in the same PFA solution for fixation (24 h, 4°C). The samples were transferred to a 30% sucrose solution for dehydration (48 h, 4°C). After that, the brain samples were imbedded and frozen (− 80°C), and then sliced into coronal slices (20 μm thick) which were mounted on glass slides. Before staining, the slides were washed with PBS and processed with a mixture of Triton X-100 (0.3%) and 3% BSA (Sigma A7906) for 1 h. Next, the slides were incubated with primary antibodies overnight (24 h, 4°C). Then, the corresponding secondary antibodies were added and allowed to co-incubation (1 h, 24°C). Afterwards, the slides were washed and sealed with a DAPI reagent (Thermo Fisher, MA, USA) and subsequently examined under a fluorescence microscope (Leica,

Germany). Primary antibodies used were anti-Iba-1 (1:100; ab-178847, Abcam, MA, USA), anti-Arg1 (1:100; DF6657, Affinity, MA, USA) and anti-NOS2 (1:100; sc-7271, SANTA CRUZ, MA, USA). Secondary antibodies used were anti-rabbit (1:100; ab150077, Abcam, MA, USA) and anti-mouse (1:100; ab150117, Abcam, MA, USA).

2.8 Isolation of brain microglial cells

Microglial cells, major inflammatory innate immune cells in the CNS, were isolated by collagenase digested from the mice brain tissues as previously described[28]. Briefly, brain tissue was minced with scalpels prior to digestion with 10ml of 0.25% (weight by volume) collagenase IV (Sigma, San Francisco, USA) and 20μL DNase Ⅰ (28 U/mL Sigma, D5025, San Francisco, CA, USA) for 20 min while rotating at 37°C. Subsequently, the digested tissues were collected, mashed, and filtered through a 200-mesh nylon membrane (Sigma-Aldrich, S3895, Oakville, ON, Canada). The homogenate was centrifuged for 7 min at 421 × g, and then the supernatant was carefully poured off and discarded. Myelin was removed by centrifugation of homogenates resuspended with 37% Percoll (Solarbio Technology, Beijing, China) for 10 minutes at 500 × g, without brakes. The myelin layer and the supernatant were aspirated and the pellet was kept. Following this, the cells were washed with 1× Hank's Balanced Salt Solution (HBSS) and centrifuged for 10 min at 550 × g. The resulting cell pellet was washed twice with Dulbecco modified Eagle medium (DMEM) before resuspension. Finally, cells were then resuspended at a concentration of 1 × 10^7 per ml and subjected to staining for flow cytometry.

2.9 Flow cytometry analysis

All flow cytometry staining steps were performed at 4°C in the dark. To prevent non-specific binding, cells were incubated for 20 min with 1 μL CD16/CD32 (No. 214228, BD Biosciences, USA) to block Fc receptors. Subsequently, 100 μL of suspended cells were stained with PE-conjugated anti-mouse CD45 antibody and APC-conjugated anti-mouse CD11b antibody (No. 553081, BD Biosciences, No. 553312, USA) for 30 min. Meanwhile, cells were stained with corresponding isotype control antibodies. Finally, the prepared samples were analyzed using Cyto FLEX flow cytometer (Beckman Coulter, USA).

2.10 Enzyme-linked immunosorbent assay (ELISA)

TNF-α, IL-1β, IL-6, IL-18 and IL-10 were measured by ELISA (R&D Systems, Minneapolis, MN) in the hippocampus and prefrontal cortex. Briefly, isolation of hippocampus and prefrontal cortex from fresh mice brain tissue rinsed with cold saline. Then, they were weighed, and homogenized on PBS. To obtain the cytokine supernatant, the homogenates were centrifuged for 5 min at 10,000 × g. Cytokine levels in the hippocampus or prefrontal cortex were determined by ELISA with commercial reagent kits following the manufacturer's instruction (Cloud-Clone Corp, China). The absorbance at 450 nm was determined using a microplate reader (Varioskan LUX, Thermo Fisher Scientific, USA), and the OD value was recorded for further evaluation.

2.11 Reverse transcription-quantitative (RT-q) PCR

Total RNA was extracted from the hippocampus and cortical tissue using an RNA simple Total RNA kit (Servicebio, Wuhan, China), and the SweScript RT I First Strand cDNA Synthesis Kit (Servicebio, Wuhan, China) was used to synthesize cDNA.Then, RT-qPCR was performed using the SYBR Green RT-qPCR system (SYBR-Green; Servicebio, Wuhan, China) according the manufacturer's protocol. The sequences for the primers were as follows:

NF-κB p65-F: 5'-CGAGTCTCCATGCAGCTACG-3',

NF-κB p65-R: 5'-TTTCGGGTAGGCACAGCAATA-3';

PPAR-γ-F: 5'-GACCACTCGCATTCCTTTGACA-3',

PPAR-γ-R: 5'-ATCGCACTTTGGTATTCTTGGA-3';

GPR109A-F: 5'-TCAGGTGGCACGATGCTATG-3',

GPR109A-R: 5'-GAGGAGTAGATGTCACAGTTGCG-3';

GAPDH-F: 5'-CCTCGTCCCGTAGACAAAATG-3',

GAPDH-R: 5'-TGAGGTCAATGAAGGGGTCGT-3'.

All primers were purchased from Servicebio. For relative quantification, the reaction conditions were in accordance with the manufacturer's instructions: initial denaturation at 95°C for 3 min, followed by 40 cycles of denaturation at 95°C for 10 sec, annealing at 60°C for 40 sec and extension at 72°C for 30 sec; iQ™5 software (Bio-Rad Laboratories, Inc.) was used to conduct PCR amplification. The RNA expression levels were evaluated using the $2^{-\Delta\Delta}$Cq method[29]. PRISM 8 soft-ware (GraphPad Software, Inc.) was used to evaluate the relative RNA level. All measurements were carried out 3 times (three independent experiments).

2.12 Western Blot

Mice hippocampus and cortical tissue were lysed by RIPA buffer (125 mM NaCl, 25 mM TRIS-Cl pH 7.4, 1 mM EGTA-TRIS pH 7.4, 1% Triton-X100, 0.5% sodium deoxycholate, 0.1% SDS and Complete EDTA-free protease inhibitor mixture (Roche Applied Science)) on ice for 30 min and blow and beat the spearhead every 10 min during this period. The protein concentrations were determined by BCA Protein Assay Kit (Pierce) and denatured by boiling for 5 min. Equal amounts of protein (40-60 μg per lane) were separated by 10% SDS-PAGE and gels were transferred onto 0.45 μm nitrocellulose membranes (Bio-Rad, Richmond, CA) under wet transfer conditions using 1× Transfer Blotting Buffer (Boston Bio Products) with 30% methanol for 40 min at a constant 220 MA. After transfer, the membrane was blocked with 0.1% BSA in TBST for 1 h and then probed with the rabbit monoclonal PPAR-γ antibody (1:1000, ab272718, Abcam), the mouse monoclonal NF-κB p65 (1:1000, sc-8008, Santa Cruz), the mouse monoclonal GPR109A (1:1000, sc-377292, Santa Cruz) and mouse monoclonal β-Actin (1:1000, ab8226, Abcam) in the blocking

solution (PBS at 0.1 M with 5% w/v non-fat dry milk) overnight at 4°C. After three washes with PBS/0.05%-Tween 20, the membrane was incubated for 1.5 h in the blocking solution at room temperature with the goat anti-mouse IgG 800RD (1:5000, cat. No. 926-32210, BD Biosciences) or goat anti-rabbit IgG 680RD (1:5000, cat. No. 925-68071, BD Biosciences). Finally, Odyssey CLX software (9141-00; BD Biosciences) was used for imaging and the lanes were analyzed by Image J.

2.13 Statistical analysis

GraphPad Prism version 8 (GraphPad Software Inc., La Jolla, CA, USA) and the statistical package for the social sciences (SPSS) 23.0 software (IBM Inc., Armonk, NY, USA) were used for statistical analyses. All data were checked for normality and homogeneity of variance using the Shapiro-Wilk and Levene tests, respectively. Data were expressed as mean ± standard error. The differences among multiple comparisons were analyzed using two-way analysis of variance followed by the Tukey multiple comparison test. Difference between the two groups was assessed using student's *t* test (two-tailed). Body weight, MWM test and shuttle-box test recorded consecutively were analyzed using repeated measure ANOVA following Tukey's multiple comparisons test. For data analysis that did not meet the normality and homogeneity of variance tests, nonparametric tests were used. $P < 0.05$ was considered a statistically significant difference.

3. Results

3.1 Sodium butyrate alleviated aberrant behaviours of mice in chronic alcohol exposure.

We investigated the efficacy of sodium butyrate supplementation on cognitive function using 4 established learning and memory tests: NOR, MWM, Y-maze and shuttle-box tests. Consistent data were obtained from above 4 independent experiments.

In the NOR (Fig. 1A), alcohol-fed mice failed to recognize novel object, spending significantly more time the familiar object than the novel object, compared with the control group, indicating excessive alcohol consumption impaired object recognition memory. Importantly, after the intervention with sodium butyrate, cognitive function with respect to the frequency of touching the novel object was significantly recovered (Fig. 1D).

In the MWM test (Fig. 1B), mice were trained over a period of 6 days to swim to a hidden, submerged platform using visual cues. The average latency to find the platform decreased over the training period for all groups, while the average latency for alcohol mice only decreased slightly and was significantly different when compared to other three groups (Fig. 1F). On the last training day (day 6), we analyzed the latency to target among the 4 groups. Mice in the AF/CON group took a significantly longer time to locate the escape platform than that in control group, indicating impaired learning memory in chronic alcohol exposure. AF mice with the NaB intervention located the platform in a much quicker manner (Fig. 1I).

Furthermore, in the space exploration experiment, mice in the AF/CON group crossed the platform considerably with less number of times compared to the PF/CON group, suggesting diminished in spatial recognition memory. Meanwhile, dietary NaB supplementation increased numbers of the platform cross for improving the recognition memory (Fig. 1J).

Y-maze test was continuously used to assess the impact of alcohol exposure and subsequent sodium butyrate intervention on spatial learning and memory. As showed in the heat maps (Fig. 1C), generally, rodents investigated a new arm of the maze (target arm) rather than returning to the two that were accessible (start arm and known arm). Examining the entire 5-min scoring, mice with chronic excessive alcoholic exposure spent more time. However, mice in the AF/NaB group exhibited more preference to the target arm (Fig. 1E), suggesting sodium butyrate could effectively attenuate impaired spatial learning and memory induced by chronic alcohol consumption.

In addition, the shuttle-box was recorded active avoidance in mice to evaluate learning ability. Notably, decreased times of active avoidance were observed in the AF/CON group, which was conversely attenuated with sodium butyrate intervention (Fig. 1G). We also continuously recorded the times of active avoidance among 5 days of training (Fig. 1H). These results revealed that the impairment of the memory cognitive functions induced by chronic alcohol consumption could be improved by sodium butyrate intervention.

Apart from the above tests to evaluate memory and cognition, we conducted the OFT (Fig. 1K) and FST (Fig. 1L) for the assessment of locomotor activity, anxiety, and exploratory behavior. In the OFT, mice in AF/CON group spent less time in the inner zone, less total travelled distance and less rearing than those in PF/CON group (Fig. 1M, N and O). In the FST (Fig. 1L), immobility time in the AF/CON group was extended (Fig. 1P), indicating that the increased anxiety-like and depression-like behaviors caused by chronic alcohol exposure, but dietary sodium butyrate reduced immobility time and increased the center time, total distance and number of rears during alcohol exposure, which revealed that sodium butyrate may regulate anxiety-like and depression-like behaviors.

Collectively, these behavioural tests demonstrated that mice with chronic excessive alcoholic consumption displayed locomotor hypoactivity, anxiety disorders and depressive-like behaviors, impaired learning and spatial recognition memory. Intriguingly, sodium butyrate intervention was demonstrated to improve these abnormal behaviours .

3.2 Physical parameters in the different groups of mice.

The body weights (BWs) of the indicated groups were continuously monitored during the modeling and administration periods (6 weeks). Similar BWs were observed in all groups at the initiation of the study. The BWs in AF/CON group were dramatically decreased in week 2 ($p < 0.05$), week 3 ($p < 0.01$), week 4 ($p < 0.01$), week 5 ($p < 0.001$) and week 6 ($p < 0.001$), compared to PF/CON group. Interestingly, during 6 weeks of sodium butyrate intervention after modelling, there were significant differences in the BWs between the AF/CON and AF/NaB groups at week 4 ($p < 0.05$), week 5 ($p < 0.001$), and week 6 ($p < 0.001$),

indicating that sodium butyrate intervention affected BWs in alcohol mice. (Fig. 2A). Similarly, brain-to-body mass ratio was decreased in the AF/CON group ($p < 0.01$), which could be reversed by butyrate supplementation ($p < 0.05$) (Fig. 2B).

3.3 Sodium butyrate attenuated the brain physiology and pathomorphology injury in chronic alcohol exposure.

To further confirm the pathological changes and neuronal degeneration in the brain, HE staining, Nissl staining, and immunohistochemistry were performed respectively. First, HE staining showed that the hyperchromatic nuclei and severe inflammatory cell infiltration in the AF/CON group compared to the PF/CON group, whereas 6 weeks of sodium butyrate intervention distinctly alleviated the brain histopathological injury (**Fig. S1**). Moreover, mice in the AF/CON group showed the loss and necrosis of neurons with nucleus condensation, cell shrinkage, nuclear envelope shrinkage, chromatin condensation to nuclear envelope, irregular condensation in various regions of the hippocampus (CA1, CA3 and DG) as opposed to PF/CON group. When treated with sodium butyrate, we found the nuclear hyperchromatism was reduced, suggesting that neuronal damage was alleviated. A similar result was seen in the prefrontal cortex (Fig. 3). Further, we observed exhibited enlarged hepatocytes and extensive vacuolization of liver in the AF/CON group, but these changes were ameliorated in the AF/NaB group (**Fig. S2**).

It was noteworthy in this experiment the protective role of sodium butyrate in chronic alcoholic nerve damage. To test whether the effectiveness were attributed to the suppression of inflammation, the following experiments were performed.

3.4 Sodium butyrate significantly reduced neuroinflammation in chronic alcohol exposure.

First, we performed the immunohistochemistry in the hippocampus and prefrontal cortex, the microglia marker Iba-1 displayed a brown colour (Fig. 4A-B). In the hippocampal DG, CA1 and CA3 areas, microglial cells in the AF/CON group were significantly higher and larger with increased synaptic branches than those in the PF/CON group (all $p < 0.0001$). By contrast, treatment with sodium butyrate in AF mice, we found that the number of positive cells was decreased, as well as the morphology was changed between active and resting status ($p < 0.0001$, $p < 0.001$ and $p < 0.0001$, respectively) (Fig. 4C-E). The same trend can be seen in the prefrontal cortex (Fig. 4F) ($p < 0.0001$).

Similarly, the Iba-1 immunofluorescence of the hippocampus (DG, CA1 and CA3) and prefrontal cortex was corroborated with the above immunohistochemistry results (Fig. 5A). In the DG, CA1 and CA3 areas, the Iba-1 fluorescence intensity was increased in the AF/CON group compared to the PF/CON group ($p < 0.0001$, $p < 0.0001$, $p < 0.01$, respectively). Similar effects in the cortical area were observed ($p < 0.0001$). On the contrary, the Iba-1 fluorescence of the AF/NaB group was notably decreased ($p < 0.0001$, $p < 0.01$, $p < 0.001$ and $p < 0.0001$, respectively) (Fig. 5B **- E**).

Moreover, flow cytometry was performed to detect microglia cells among 4 groups (Fig. 6A). The proportions of $CD45^{+}CD11b^{+}$ microglial cells were increased in the AF/CON group compared to the PF/CON group ($p < 0.0001$), which were decreased in treatment with sodium butyrate ($p < 0.001$) (Fig. 6B).

Taken together, these results demonstrated that the excessive proliferation and activation of microglial cells induced by chronic alcoholic abuse could be effectively rectified by sodium butyrate intervention.

3.5 Sodium butyrate regulated M1/M2 microglia polarization in chronic alcohol exposure.

To further evaluate the effects of sodium butyrate on the polarization of microglia in alcoholic neuroinflammation, we examined the types of microglia M1/M2 polarization in the hippocampus (DG, CA1 and CA3) and prefrontal cortex using immunofluorescence (Fig. 7A-D). In the DG, CA1 and CA3 regions, the results showed that the optical density of iNOS was increased (all $p < 0.0001$) but Arg-1 was decreased ($p < 0.0001$, $p < 0.0001$ and $p < 0.001$, respectively) in the AF/CON group compared to the PF/CON group. However, sodium butyrate intervention notable changed these abnormal iNOS (all $p < 0.0001$) and Arg-1 (all $p < 0.0001$). The same iNOS and Arg-1 results were observed in the prefrontal cortex. Collectively, sodium butyrate may play an anti-inflammatory role by regulating microglia polarization.

3.6 Sodium butyrate suppressed the inflammation by regulating the inflammatory factors in chronic alcohol exposure.

Consistent with the activation of microglia cells, immune inflammatory indicators in the hippocampus and prefrontal cortex were further determined. In the hippocampus (Fig. 8A), the levels of pro-inflammatory TNF-α, IL-1β, IL-6, and IL-18 in the AF/CON group were significantly elevated in AF group ($p < 0.05$, $p < 0.0001$, $p < 0.0001$ and $p < 0.001$, respectively), as well as anti-inflammatory IL-10 was downregulated ($p < 0.001$). As expected, after sodium butyrate intervention, the inflammatory damage caused by excessive chronic alcohol abuse was relieved (Fig. 8B).

3.7 Sodium butyrate attenuated neuroinflammation by GPR109A / PPAR-γ / NF-κB signaling pathway in chronic alcohol exposure.

To clarify the mechanism of anti-inflammatory effects of sodium butyrate, the transcriptional expression levels of GPR109A receptors, PPAR-γ, and NF-κB p65 in the hippocampus were measured. GPR109A and PPAR-γ were significantly decreased in the AF/CON group compared to the PF/CON group (all $p < 0.0001$), whereas the NF-κB was increased ($p < 0.0001$), which were notably alleviated by sodium butyrate intervention (Fig. 9A-C) (all $p < 0.0001$). Moreover, similar results were also presented in the prefrontal cortex (Fig. 9D-F) .

The protein expressions of NF-κB p65, PPAR-γ and GPR109A were also respectively determined in hippocampus and cortex (Fig. 9G-N). As shown, the reductions in GPR109A and PPAR-γ ($p < 0.01$ and $p < 0.0001$), and elevated NF-κB p65 ($p < 0.0001$) were observed with AF in the hippocampus, compared to PF/CON group. Intriugingly, NaB administration alleviated the expression levels of GPR109A, PPAR-γ and NF-κB p65. A similar result was observed in the prefrontal cortex. These data indicated that sodium butyrate attenuated chronic alcoholic neuroinflammation via GPR109A / PPAR-γ / NF-κB pathways.

4. Discussion

Alcohol is consumed worldwide, and drinking alcohol is a common part of many cultures. But alcohol consumption can cause neurocognitive and behavioral damage, and neuroinflammation may be an important reason. In the present study, our results demonstrated that sodium butyrate alleviated chronic alcoholic neuroinflammation. The beneficial effects may be due to the suppression of M1 and facilitation of M2 microglia to inhibiting the release of inflammatory indicators by modulating GPR109A-PPAR-γ-NF-κB axis. This intervention exerted potential preventive and therapeutic value.

Alcoholism and alcohol poisoning of the brain have become international concern with harmfulness associated with marked abnormalities in cognitive and motor abilities, including impaired judgment, blunted affect, social withdrawal, reduced motivation, distractibility, and attention[30, 31]. More researches have shown that accumulating progressive alcohol consumption leads to alterations in brain structure that reduce behavioral control, promoting further alcohol abuse and neurodegeneration[32, 33]. Human epidemiological studies have demonstrated alcoholics with cognitive dysfunction, including marked impairment in spatial learning and short-term and long-term memory[34, 35]. In this study, a variety of behavioral tests demonstrated that chronic alcohol consumption led to a deleterious influence on emotional behavior and cognition, which was consistent with previous human and animal studies. However, the improvements of emotion, cognition and memory functions in the AF/NaB group suggested that sodium butyrate could attenuate the depression and anxiety-like behavior and damage of cognition functions .

Neuroinflammation is one of the mechanisms of neurodegeneration caused by chronic alcohol exposure[36]. There is overwhelming evidence for distinct changes in multiple pro-inflammatory cytokines after alcohol exposure. The effects of alcohol consumption on the function of the immune system via synthesis of pro-inflammatory cytokines have been reported[37, 38]. In another study, an alcohol ingestion induced increase in inflammatory cytokines including TNF-α and IL-1β[39]. Increased levels of TNF-α activate NF-κB and in turn promote the production of pro-inflammatory IL-6 and IL-1β[40]. This may activate microglial cells, and increase neuroexcitatory activity, ultimately leading to neurodegenerative effects[41]. The response of anti-inflammatory IL-10 in brain could inhibits pro-inflammatory cascades, thus contributing to protection against alcohol exposure[42]. Our results showed that TNF-α, IL-6, IL-1β and IL-18 levels of the hippocampus and prefrontal cortex tissues in the AF/NaB group were significantly decreased and IL-10 was increased, demonstrating that sodium butyrate

alleviated neuroinflammation mainly by reducing pro-inflammatory cytokines and elevating anti-inflammatory cytokines.

It is well known that microglial activation is associated with neuroinflammation and pathology of various neurodegenerative diseases[43]. Chronic alcohol consumption induced microglia activation in the CNS, particularly in the hippocampus[44]. With continued activation of microglia, prolonged production of inflammatory mediators by microglia may result in chronic inflammation and implicated in further tissue damage[45]. In this study, the immunohistochemistry, immunofluorescence and flow cytometry of microglia in the prefrontal cortex and hippocampus all demonstrated that sodium butyrate could effectively reverse the excessive activation of microglia and protect neurons from damage by reducing the release of inflammatory cytokines. M1/M2 polarization plays a critical role in microglia-mediated neuroinflammation[46]. M1 microglia expresses high levels of pro-inflammatory iNOS and TNF-α, whereas M2 microglia induces anti-inflammatory Arg-1 and IL-10[47]. Thus, the effects of sodium butyrate on microglia M1/M2 polarization were investigated by subsequently detecting the proportions of iNOS and Arg-1 in the hippocampus and cortex of chronic alcohol exposed mice. An elevation of Arg-1 and a reduction of iNOS in DG, CA1,CA3 and prefrontal cortex areas after treatment of sodium butyrate revealed that sodium butyrate may alleviate the neuroinflammation by suppressing M1 and activating M2. This is consistent with the effect of sodium butyrate on the polarization of liver macrophages in our research group on ALD.

Moreover, NF-κB is a critical transcription factor that controls the expression of genes encoding pro-inflammatory cytokines, inducible inflammatory enzymes such as iNOS and immune receptors[48]. A recent study demonstrated that butyrate treatment reduced CD11b and inhibited phosphorylation of NF-κB p65 in BV2 microglia[49]. In addition to inhibition of NF-κB activation, butyrate may also exert an anti-inflammatory activity by up-regulating PPAR-γ by binding to GPR109A[50]. Elevations of GPR109A, PPAR-γ and a reduction of NF-κB p65 after treatment of sodium butyrate revealed that sodium butyrate may alleviate the neuroinflammation through GPR109A / PPAR-γ / NF-κB signaling pathway.

Chronic alcohol exposure induces a complex response with activation of a variety of immune responses and inflammatory expression. In the present study, anti-inflammatory sodium butyrate may contribute to the potential therapy for the chronic alcoholic neuroinflammation via modulating M1/M2 balance. However, the relationship of butyrate with other immune cells such as T cell-mediated inflammatory response in chronic alcoholic neuroinflammation still needs to be further investigated.

5. Conclusions

In summary, sodium butyrate alleviated neuroinflammation of chronic alcohol through suppressing M1 and facilitating M2 relating to GPR109A / PPAR-γ / NF-κB pathway in mice, thus ameliorating cognitive decline and emotional behavior changes, which may contribute to serving as an inexpensive intervention for the prevention and treatment of neuroinflammation associated with chronic alcoholic patients.

Abbreviations

WHO
World Health Organization
CNS
Central nervous system
ALD
Alcoholic liver disease
TNF-α
Tumor necrosis factor-α
IL-1β
Interlukin-1β
IL-6
Interlukin-6
iNOS
Nitric oxide synthase
Arg1
Arginase-1
NF-κB
Nuclear factor-κB
PPAR-γ
Peroxisome proliferator-activated receptorγ
SCFAs
Short chain fatty acids
Mψ
Macrophage
GPR109A
G-protein coupled receptor 109A (GPR109A)
LDL
Low-density lipoprotein
PF/CON
Pair-fed (PF) group
AF/CON
Alcohol-fed (AF) group
PF/NaB
PF with sodium butyrate
AF/NaB
AF with sodium butyrate
MWM
Morris water maze

NOR
New object recognition
OFT
Open field test
FST
Forced swim test
HE staining
Hematoxylin and eosin staining
IHC staining
Immunohistochemistry staining
IF staining
Immunofluorescence staining
RT-qPCR
Reverse transcription-quantitative polymerase chain reaction
BW
body weight

Author contributions

Declarations

Author contributions

Conceptualization, J.L, H.W., HL.W., and XX.Z; methodology, Y.R., CY.Y., HL.W.,

C. Z., L.G., T.W. and FF.C.; software, HL.W. and CY.Y.; validation, J.L., H.W., HL.W. and XX.Z.; data analysis, HL.W., C.Z., CY.Y.; writing—original draft preparation, HL.W. and Y.R.; writing—review and editing, H.W. and HL.W.; supervision, J.L., H.W., XX.Z.; project administration, H.W.; funding acquisition, J.L. All authors have read and agreed to the published version of the manuscript.

Funding

This work was supported by the National Natural Science Foundation of China (Grant No. 82060238, 82160691) and Ningxia Natural Science Foundation, China (Grant No. 2022AAC02026, 2021AAC05010).

Availability of data and materials

The datasets of the current study are available from the corresponding author on reasonable request.

Acknowledgements

The authors are grateful to the Ningxia Key Laboratory of Cerebrocranial Disease of Ningxia Medical University for their kind help on technical expertise.

Ethics approval and consent to participate

All animal experiments were approved by the Animal Ethics Committee of Ningxia Medical University and were performed in accordance with the protocol and requirements of the Animal Ethics Committee of Ningxia Medical University (2019-137).

Consent for Publication

Not applicable.

Competing interests

The authors report no conficts of interest in this work.

References

1. Meroni M, Longo M, Dongiovanni P. Alcohol or Gut Microbiota: Who Is the Guilty? INT J MOL SCI. 2019;20(18).
2. Socodato R, Henriques JF, Portugal CC, Almeida TO, Tedim-Moreira J, Alves RL, et al. Daily alcohol intake triggers aberrant synaptic pruning leading to synapse loss and anxiety-like behavior. SCI SIGNAL. 2020;13(650).
3. King JA, Nephew BC, Choudhury A, Poirier GL, Lim A, Mandrekar P. Chronic alcohol-induced liver injury correlates with memory deficits: Role for neuroinflammation. ALCOHOL. 2020;83:75–81.
4. Fuenzalida C, Dufeu MS, Poniachik J, Roblero JP, Valenzuela-Perez L, Beltran CJ. Probiotics-Based Treatment as an Integral Approach for Alcohol Use Disorder in Alcoholic Liver Disease. FRONT PHARMACOL. 2021;12:729950.
5. Rodriguez-Gonzalez A, Orio L. Microbiota and Alcohol Use Disorder: Are Psychobiotics a Novel Therapeutic Strategy? Curr Pharm Des. 2020;26(20):2426–37.
6. Keresztes A, Raffington L, Bender AR, Bogl K, Heim C, Shing YL. Hair cortisol concentrations are associated with hippocampal subregional volumes in children. Sci Rep. 2020;10(1):4865.
7. Tesfaye G, Demlew D, G TM, Habte F, Molla G, Kifle Y, et al. Correction to: The prevalence and associated factors of alcohol use among pregnant women attending antenatal care at public hospitals Addis Ababa, Ethiopia, 2019. BMC PSYCHIATRY. 2020;20(1):493.
8. Lowe PP, Morel C, Ambade A, Iracheta-Vellve A, Kwiatkowski E, Satishchandran A, et al. Chronic alcohol-induced neuroinflammation involves CCR2/5-dependent peripheral macrophage infiltration and microglia alterations. J Neuroinflammation. 2020;17(1):296.
9. Garcia-Baos A, Alegre-Zurano L, Cantacorps L, Martin-Sanchez A, Valverde O. Role of cannabinoids in alcohol-induced neuroinflammation. Prog Neuropsychopharmacol Biol Psychiatry. 2021;104:110054.
10. Warden AS, Wolfe SA, Khom S, Varodayan FP, Patel RR, Steinman MQ, et al. Microglia Control Escalation of Drinking in Alcohol-Dependent Mice: Genomic and Synaptic Drivers. Biol Psychiatry.

2020;88(12):910–21.

11. Nelson JC, Greengrove E, Nwachukwu KN, Grifasi IR, Marshall SA. Repetitive binge-like consumption based on the Drinking-in-the-Dark model alters the microglial population in the mouse hippocampus. J INTEGR NEUROSCI. 2021;20(4):933–43.
12. Marshall SA, Geil CR, Nixon K. Prior Binge Ethanol Exposure Potentiates the Microglial Response in a Model of Alcohol-Induced Neurodegeneration. Brain Sci. 2016;6(2).
13. Tang Y, Le W. Differential Roles of M1 and M2 Microglia in Neurodegenerative Diseases. MOL NEUROBIOL. 2016;53(2):1181–94.
14. Guo Y, Hong W, Wang X, Zhang P, Korner H, Tu J, et al. MicroRNAs in Microglia: How do MicroRNAs Affect Activation, Inflammation, Polarization of Microglia and Mediate the Interaction Between Microglia and Glioma? FRONT MOL NEUROSCI. 2019;12:125.
15. Liu JD, Bayir HO, Cosby DE, Cox NA, Williams SM, Fowler J. Evaluation of encapsulated sodium butyrate on growth performance, energy digestibility, gut development, and Salmonella colonization in broilers. Poult Sci. 2017;96(10):3638–44.
16. Sadler R, Cramer JV, Heindl S, Kostidis S, Betz D, Zuurbier KR, et al. Short-Chain Fatty Acids Improve Poststroke Recovery via Immunological Mechanisms. J NEUROSCI. 2020;40(5):1162–73.
17. Liu J, Chang G, Huang J, Wang Y, Ma N, Roy AC, et al. Sodium Butyrate Inhibits the Inflammation of Lipopolysaccharide-Induced Acute Lung Injury in Mice by Regulating the Toll-Like Receptor 4/Nuclear Factor kappaB Signaling Pathway. J Agric Food Chem. 2019;67(6):1674–82.
18. Guo C, Zhang Y, Ling T, Zhao C, Li Y, Geng M, et al. Chitosan Oligosaccharides Alleviate Colitis by Regulating Intestinal Microbiota and PPARgamma/SIRT1-Mediated NF-kappaB Pathway. MAR DRUGS. 2022;20(2).
19. Yang Z, Liu B, Yang LE, Zhang C. Platycodigenin as Potential Drug Candidate for Alzheimer's Disease via Modulating Microglial Polarization and Neurite Regeneration. MOLECULES. 2019;24(18).
20. Nyiramana MM, Cho SB, Kim EJ, Kim MJ, Ryu JH, Nam HJ, et al. Sea Hare Hydrolysate-Induced Reduction of Human Non-Small Cell Lung Cancer Cell Growth through Regulation of Macrophage Polarization and Non-Apoptotic Regulated Cell Death Pathways. Cancers (Basel). 2020;12(3).
21. Yang X, He F, Zhang Y, Xue J, Li K, Zhang X, et al. Inulin Ameliorates Alcoholic Liver Disease via Suppressing LPS-TLR4-Mpsi Axis and Modulating Gut Microbiota in Mice. ALCOHOL CLIN EXP RES. 2019;43(3):411–24.
22. Wang Z, Zhang X, Zhu L, Yang X, He F, Wang T, et al. Inulin alleviates inflammation of alcoholic liver disease via SCFAs-inducing suppression of M1 and facilitation of M2 macrophages in mice. INT IMMUNOPHARMACOL. 2020;78:106062.
23. Pluznick J. A novel SCFA receptor, the microbiota, and blood pressure regulation. Gut Microbes. 2014;5(2):202–07.
24. Hanson J, Gille A, Zwykiel S, Lukasova M, Clausen BE, Ahmed K, et al. Nicotinic acid- and monomethyl fumarate-induced flushing involves GPR109A expressed by keratinocytes and COX-2-dependent prostanoid formation in mice. J CLIN INVEST. 2010;120(8):2910–19.

25. Zandi-Nejad K, Takakura A, Jurewicz M, Chandraker AK, Offermanns S, Mount D, et al. The role of HCA2 (GPR109A) in regulating macrophage function. FASEB J. 2013;27(11):4366–74.
26. Fu SP, Wang JF, Xue WJ, Liu HM, Liu BR, Zeng YL, et al. Anti-inflammatory effects of BHBA in both in vivo and in vitro Parkinson's disease models are mediated by GPR109A-dependent mechanisms. J Neuroinflammation. 2015;12:9.
27. Zhang X, Wang H, Yin P, Fan H, Sun L, Liu Y. Flaxseed oil ameliorates alcoholic liver disease via anti-inflammation and modulating gut microbiota in mice. LIPIDS HEALTH DIS. 2017;16(1):44.
28. Guo L, Xiao P, Zhang X, Yang Y, Yang M, Wang T, et al. Inulin ameliorates schizophrenia via modulation of the gut microbiota and anti-inflammation in mice. FOOD FUNCT. 2021;12(3):1156–75.
29. Livak KJ, Schmittgen TD. Analysis of relative gene expression data using real-time quantitative PCR and the 2(-Delta Delta C(T)) Method. METHODS. 2001;25(4):402–08.
30. Sullivan EV, Rosenbloom MJ, Lim KO, Pfefferbaum A. Longitudinal changes in cognition, gait, and balance in abstinent and relapsed alcoholic men: relationships to changes in brain structure. NEUROPSYCHOLOGY. 2000;14(2):178–88.
31. Sullivan EV, Pfefferbaum A. Neurocircuitry in alcoholism: a substrate of disruption and repair. Psychopharmacology (Berl). 2005;180(4):583–94.
32. Crews FT, Collins MA, Dlugos C, Littleton J, Wilkins L, Neafsey EJ, et al. Alcohol-induced neurodegeneration: when, where and why? ALCOHOL CLIN EXP RES. 2004;28(2):350–64.
33. Wu Y, Lousberg EL, Moldenhauer LM, Hayball JD, Robertson SA, Coller JK, et al. Attenuation of microglial and IL-1 signaling protects mice from acute alcohol-induced sedation and/or motor impairment. BRAIN BEHAV IMMUN. 2011;25 Suppl 1:S155-64.
34. Beresford TP, Arciniegas DB, Alfers J, Clapp L, Martin B, Du Y, et al. Hippocampus volume loss due to chronic heavy drinking. ALCOHOL CLIN EXP RES. 2006;30(11):1866–70.
35. Sullivan EV, Pfefferbaum A. Neurocircuitry in alcoholism: a substrate of disruption and repair. Psychopharmacology (Berl). 2005;180(4):583–94.
36. Mews P, Egervari G, Nativio R, Sidoli S, Donahue G, Lombroso SI, et al. Alcohol metabolism contributes to brain histone acetylation. NATURE. 2019;574(7780):717–21.
37. Dukay B, Walter FR, Vigh JP, Barabasi B, Hajdu P, Balassa T, et al. Neuroinflammatory processes are augmented in mice overexpressing human heat-shock protein B1 following ethanol-induced brain injury. J Neuroinflammation. 2021;18(1):22.
38. Boyadjieva NI, Sarkar DK. Microglia play a role in ethanol-induced oxidative stress and apoptosis in developing hypothalamic neurons. ALCOHOL CLIN EXP RES. 2013;37(2):252–62.
39. Lippai D, Bala S, Csak T, Kurt-Jones EA, Szabo G. Chronic alcohol-induced microRNA-155 contributes to neuroinflammation in a TLR4-dependent manner in mice. PLOS ONE. 2013;8(8):e70945.
40. Rothhammer V, Mascanfroni ID, Bunse L, Takenaka MC, Kenison JE, Mayo L, et al. Type I interferons and microbial metabolites of tryptophan modulate astrocyte activity and central nervous system inflammation via the aryl hydrocarbon receptor. NAT MED. 2016;22(6):586–97.

41. Leonard B, Maes M. Mechanistic explanations how cell-mediated immune activation, inflammation and oxidative and nitrosative stress pathways and their sequels and concomitants play a role in the pathophysiology of unipolar depression. Neurosci Biobehav Rev. 2012;36(2):764–85.
42. Qin L, He J, Hanes RN, Pluzarev O, Hong JS, Crews FT. Increased systemic and brain cytokine production and neuroinflammation by endotoxin following ethanol treatment. J Neuroinflammation. 2008;5:10.
43. Do H, Bui BP, Sim S, Jung JK, Lee H, Cho J. Anti-Inflammatory and Anti-Migratory Activities of Isoquinoline-1-Carboxamide Derivatives in LPS-Treated BV2 Microglial Cells via Inhibition of MAPKs/NF-kappaB Pathway. INT J MOL SCI. 2020;21(7).
44. Shukla PK, Meena AS, Dalal K, Canelas C, Samak G, Pierre JF, et al. Chronic stress and corticosterone exacerbate alcohol-induced tissue injury in the gut-liver-brain axis. Sci Rep. 2021;11(1):826.
45. Burtscher J, Maglione V, Di Pardo A, Millet GP, Schwarzer C, Zangrandi L. A Rationale for Hypoxic and Chemical Conditioning in Huntington's Disease. INT J MOL SCI. 2021;22(2).
46. Ni L, Xiao J, Zhang D, Shao Z, Huang C, Wang S, et al. Immune-responsive gene 1/itaconate activates nuclear factor erythroid 2-related factor 2 in microglia to protect against spinal cord injury in mice. CELL DEATH DIS. 2022;13(2):140.
47. Guo Y, Hong W, Wang X, Zhang P, Korner H, Tu J, et al. MicroRNAs in Microglia: How do MicroRNAs Affect Activation, Inflammation, Polarization of Microglia and Mediate the Interaction Between Microglia and Glioma? FRONT MOL NEUROSCI. 2019;12:125.
48. Sindhu S, Kochumon S, Thomas R, Bennakhi A, Al-Mulla F, Ahmad R. Enhanced Adipose Expression of Interferon Regulatory Factor (IRF)-5 Associates with the Signatures of Metabolic Inflammation in Diabetic Obese Patients. CELLS-BASEL. 2020;9(3).
49. Sun J, Xu J, Yang B, Chen K, Kong Y, Fang N, et al. Effect of Clostridium butyricum against Microglia-Mediated Neuroinflammation in Alzheimer's Disease via Regulating Gut Microbiota and Metabolites Butyrate. MOL NUTR FOOD RES. 2020;64(2):e1900636.
50. Anand S, Kaur H, Mande SS. Comparative In silico Analysis of Butyrate Production Pathways in Gut Commensals and Pathogens. FRONT MICROBIOL. 2016;7:1945.

Figures

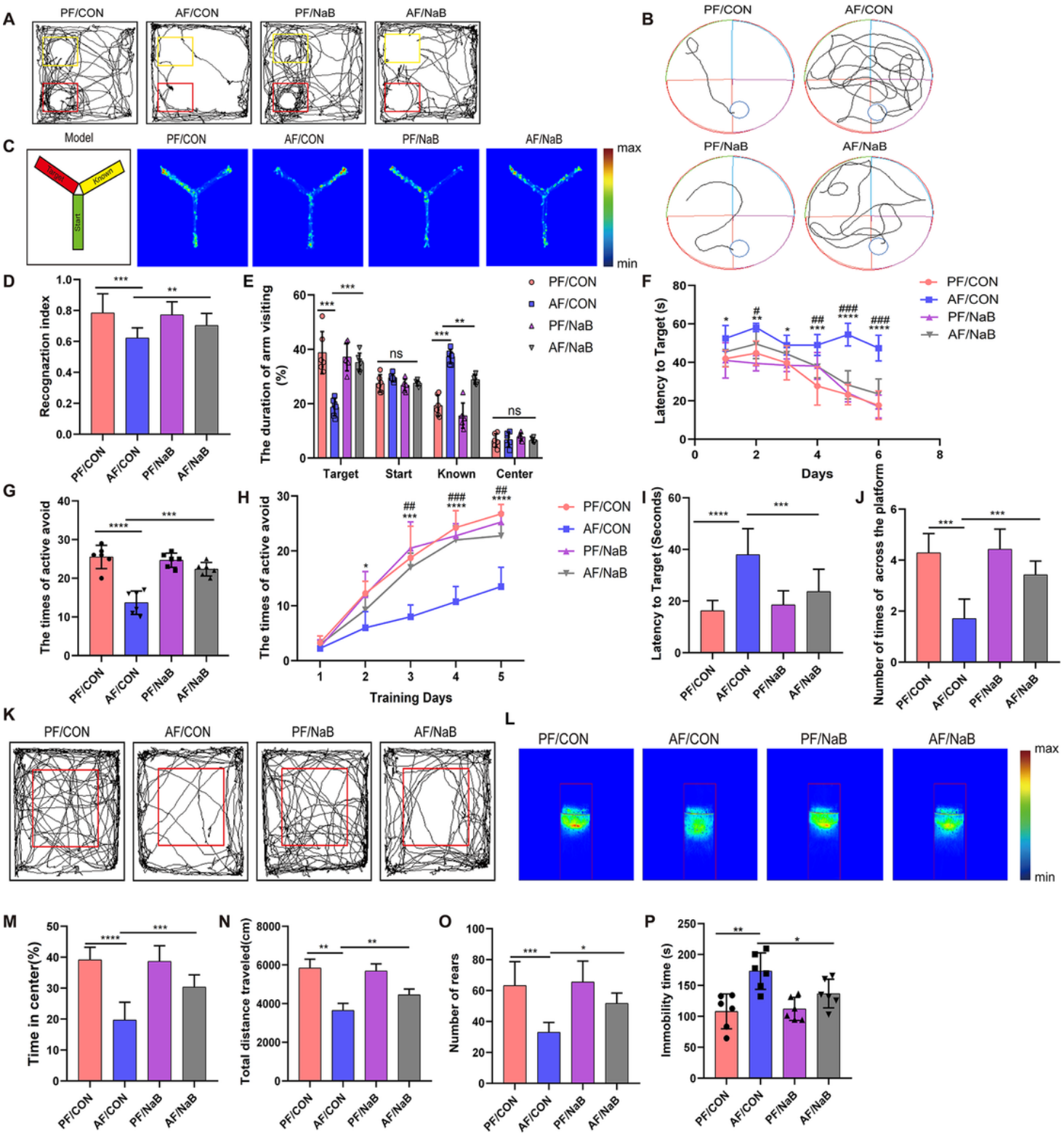

Figure 1

Behavioral changes in memory and cognitive function, decreased motor ability, depression and anxiety, and the reversal after sodium butyrate intervention in chronic alcoholic exposure mice . (A) Novel Object Recognition (NOR); (B) Morris Water Maze (MWM) test; (C) Y-maze test; (D) Recognization Index of NOR; (E) The duration of arm visiting in Y-maze test(s); (F) The time taken to reach the platform was recorded consecutively during the test period in the MWM test (s). *: AF/CON vs.PF/ CON; #: AF/NaB vs.AF/CON; (

G) Number of active avoidance in the shuttle-box test; (H) Number of active avoidance continuously recorded among 5 days of training. *: AF/CON vs.PF/ CON; #: AF/NaB vs.AF/CON; (I) The time to locate the escape platform in the MWM test(s); (J) Number of times of across the platform in the MWM space exploration test; (K) Open Field Test (OFT); (L) Forced-Swimming Test (FST); (M) The time in center in the OFT(s); (N) Total distance travelled in the OFT (cm); (O) Number of times of rears in the OFT; (P) the time of immobility was measured during 5min period in the FST(s). Data were expressed as mean ± SEM, n = 6, *$p < 0.05$, **$p < 0.01$, ***$p < 0.001$ and ****$p < 0.0001$.

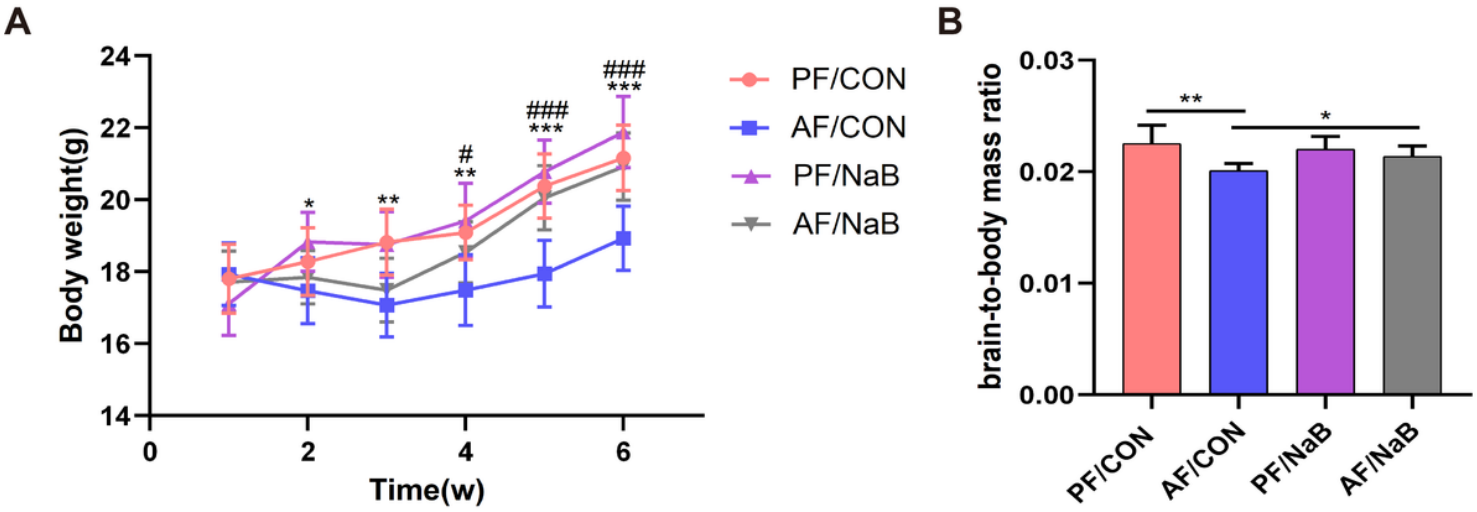

Figure 2

Physical *parameters* for *the different groups of* mice. (A) The body weights (BWs) of the indicated groups were continuously monitored during the modeling and administration periods (6 weeks); (B) The brain-to-body mass ratio. Data were presented as means ± SEM. *$p < 0.05$, **$p < 0.01$, ***$p < 0.001$ and ****$p < 0.0001$. In figure a, *: AF/CON vs.PF/ CON; #: AF/NaB vs.AF/CON.

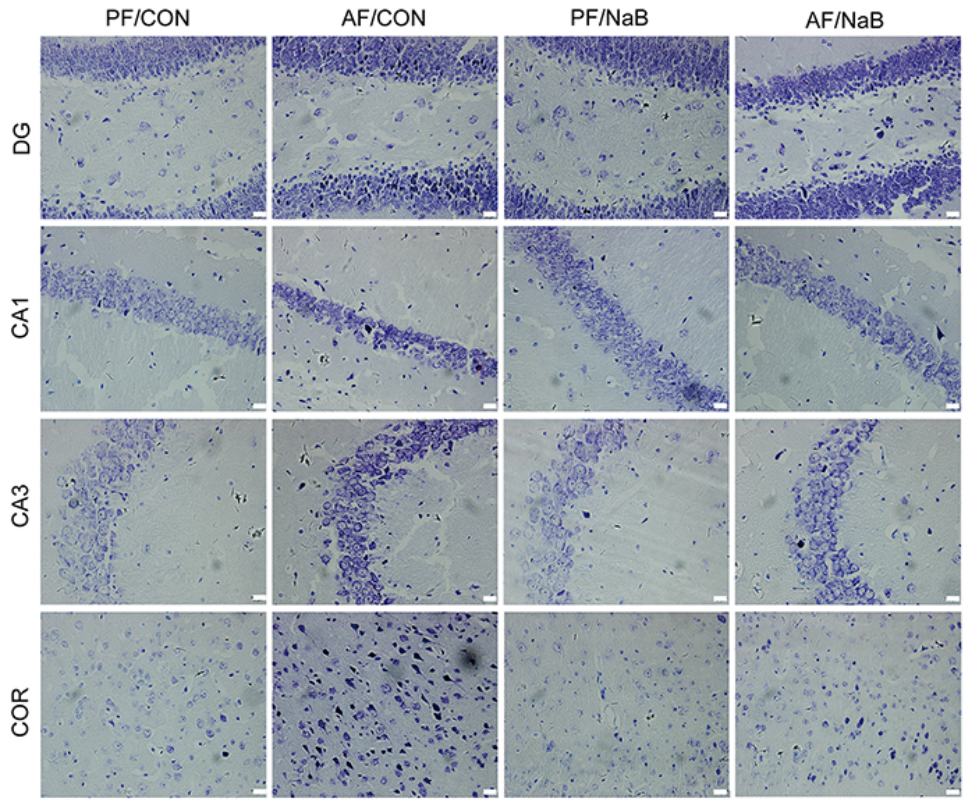

Figure 3

Sodium butyrate improved the brain physiology and pathomorphology of chronic alcohol exposed mice. Nissl staining of hippocampus (DG, CA1 and CA3) and COR, Bar = 20μm.

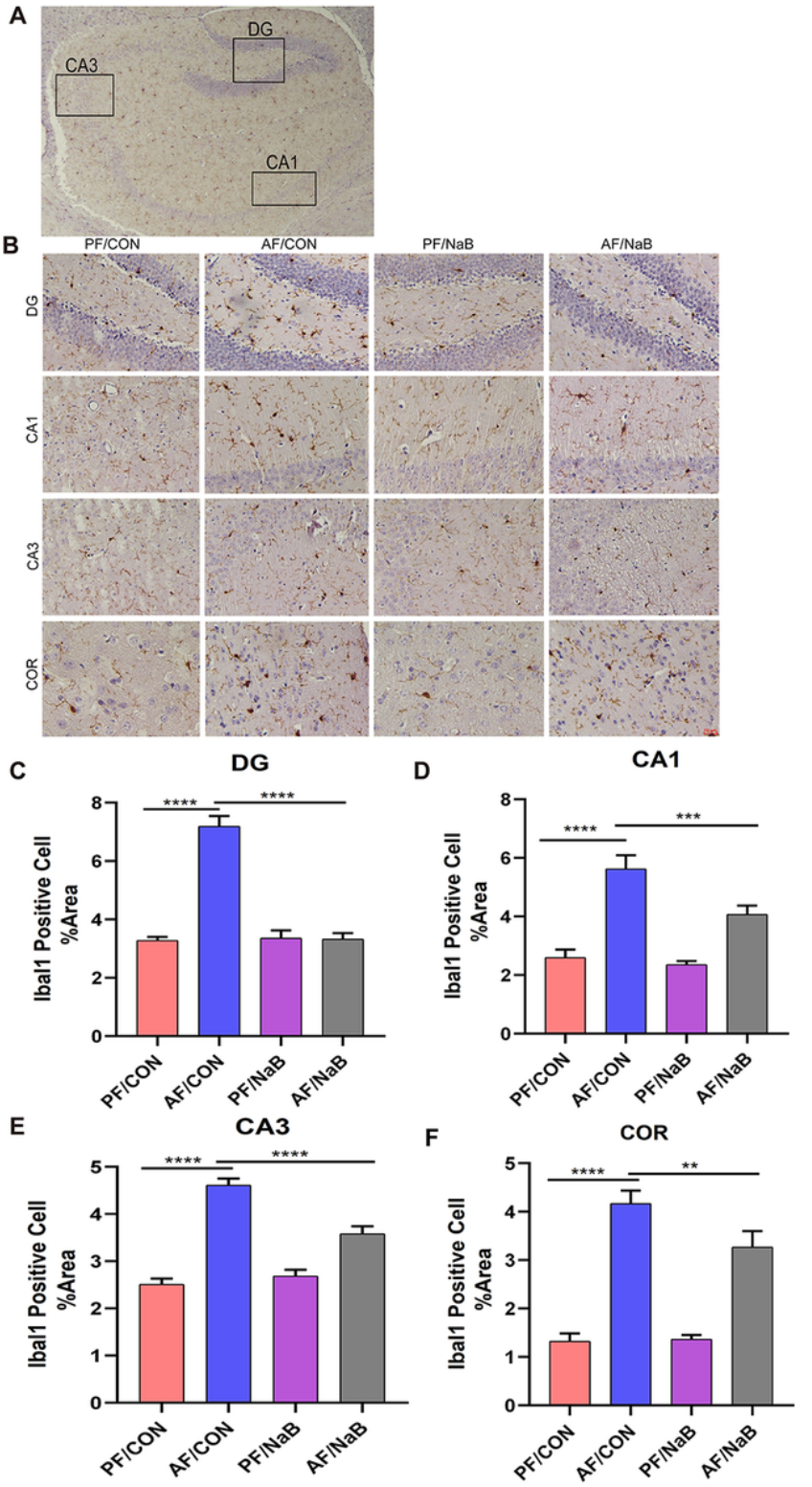

Figure 4

Sodium butyrate notably decreased the microglial expression of hippocampus in different regions (CA1, CA3 and DG) and COR of chronic alcohol exposed mice. (A) The visual map of the hippocampus showing the corresponding observation parts; (B) Immunohistochemistry (IHC) of Iba1 in hippocampus (CA1, CA3 and DG) and COR; (C) The statistical analysis of the proportion of the area occupied by positive

microglial Iba-1 cells in hippocampus (DG, CA1 and CA3) and COR of diverse groups. *$p < 0.05$, **$p < 0.01$, ***$p < 0.001$ and ****$p < 0.0001$, Bar = 10μm.

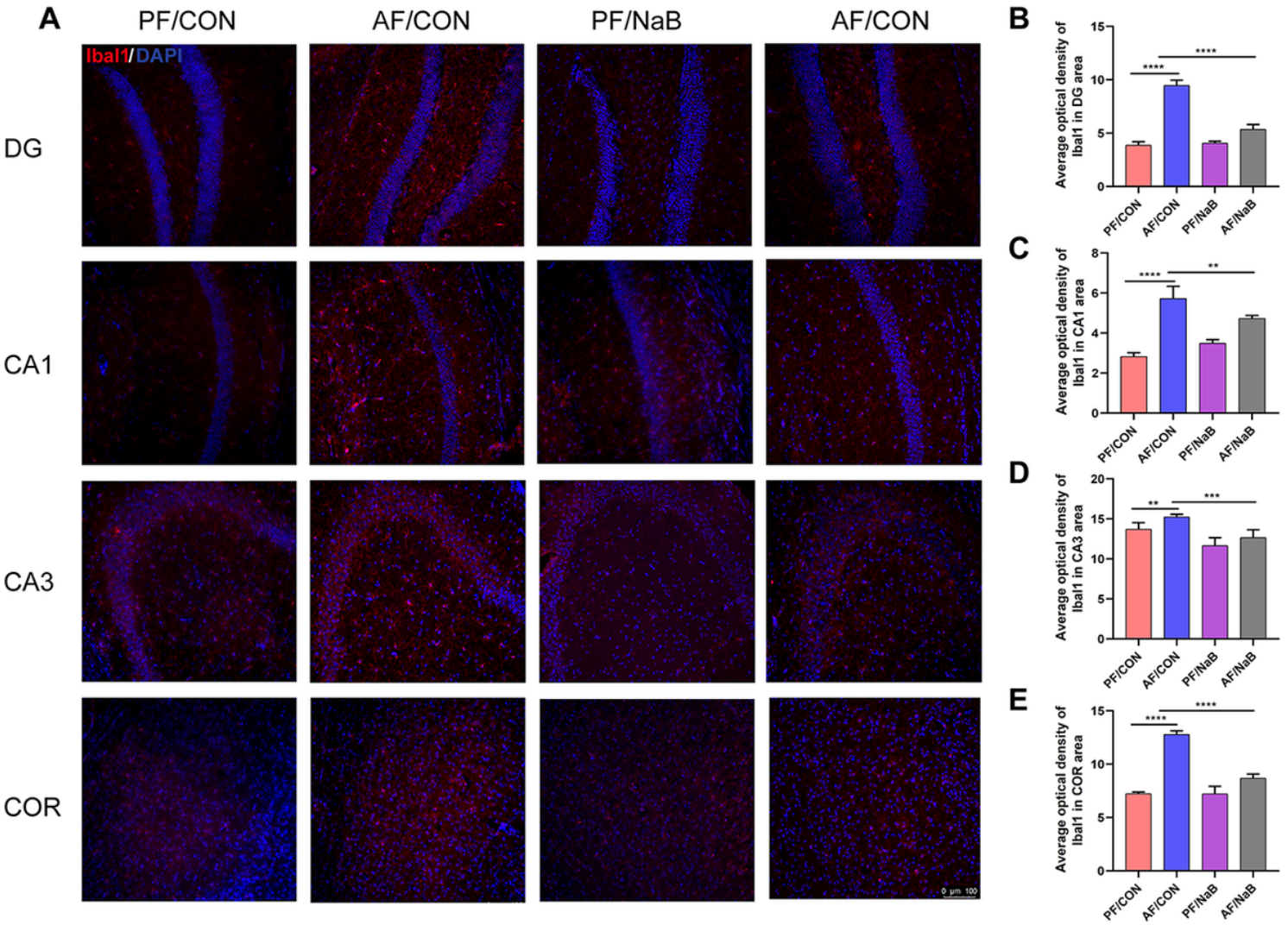

Figure 5

The Iba-1 immunofluorescence of the hippocampus (CA1, CA3 and DG) and COR. (A) The fluorescence intensity of Iba-1 in the hippocampus (CA1, CA3 and DG) and COR regions, the red is the microglia and the blue is the nucleus; (B-D) Statistical analysis of red fluorescence expression of Iba-1 in the hippocampus (CA1, CA3 and DG) and COR regions. *$p < 0.05$, **$p < 0.01$, ***$p < 0.001$ and ****$p < 0.0001$, Bar = 100μm.

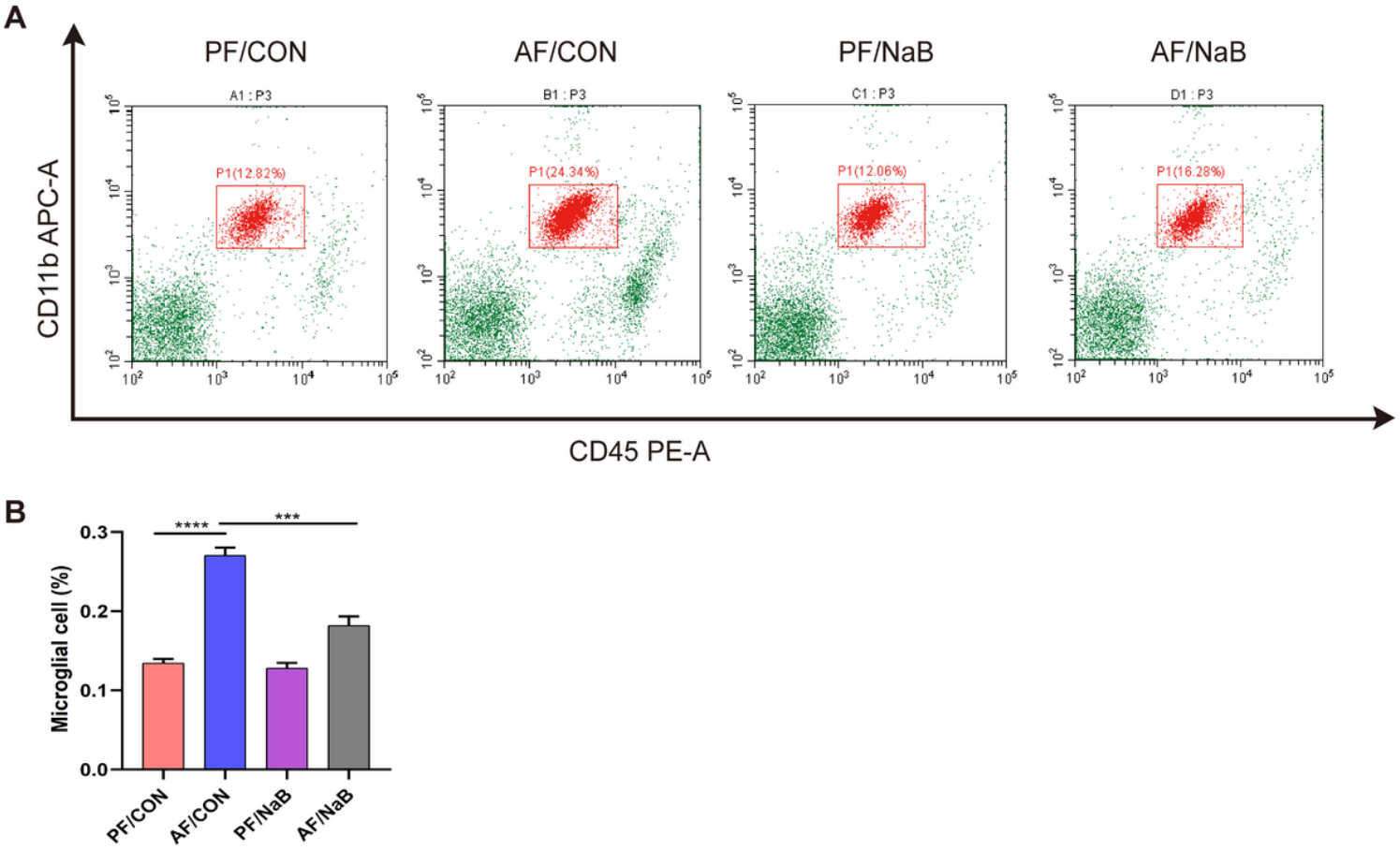

Figure 6

Further assess the effects of sodium butyrate on the proportions of microglial activation in chronic alcohol exposed mice by flow cytometry. (A) The proportions of microglia $CD11b^{+}CD45^{+}$ cells in diverse groups; (B) Flow cytometry analysis of microglia $CD11b^{+}CD45^{+}$ cells in diverse groups. *$p < 0.05$, **$p < 0.01$, ***$p < 0.001$ and ****$p < 0.0001$.

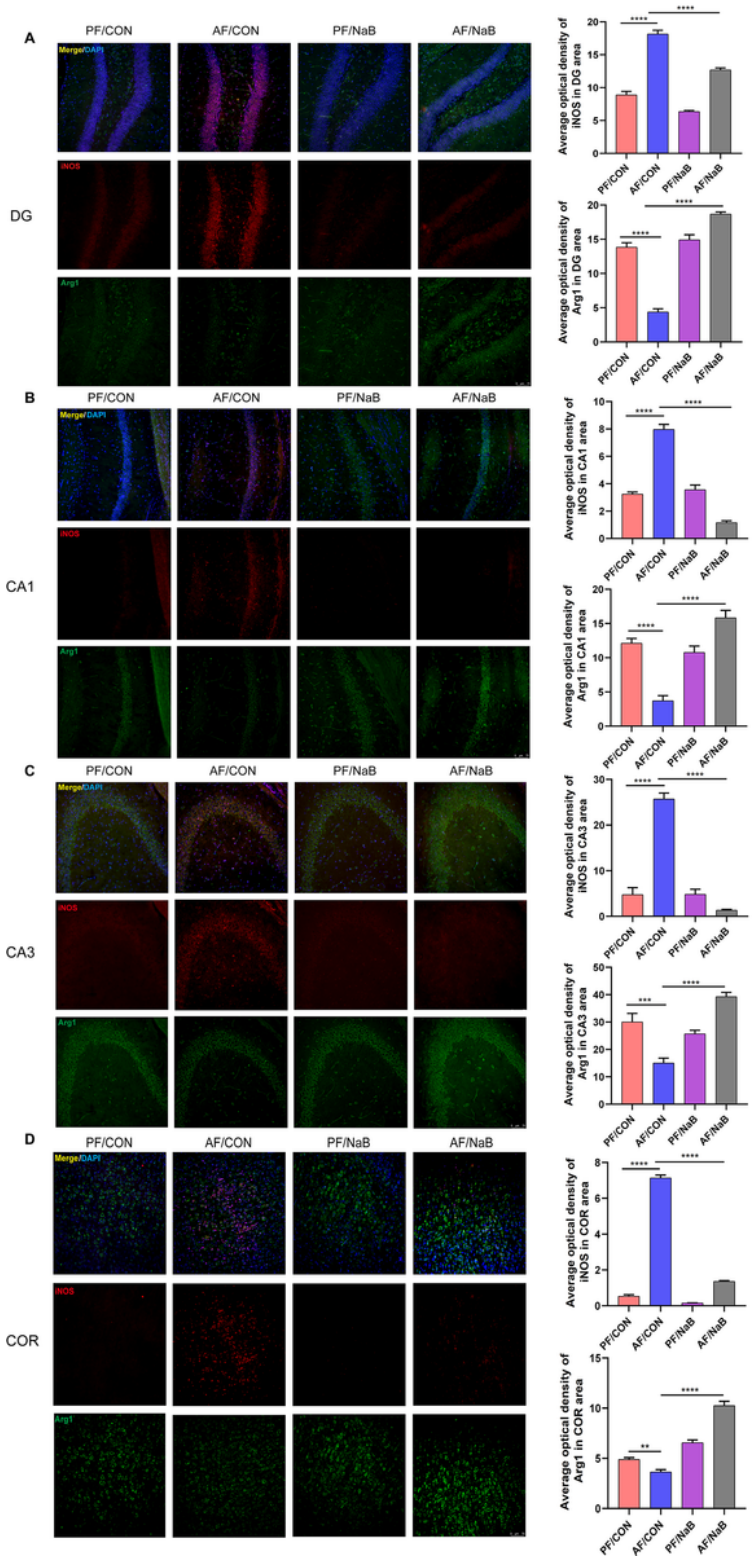

Figure 7

Sodium butyrate regulated M1/M2 microglia polarization in chronic alcohol exposure. (A) The immunofluorescence double staining for activated microglia and the analysis of expression of iNOS (M1, red) and Arg1(M2, green) in the DG region, the CA1 region (B), the CA3 region (C), the COR region (D). *p < 0.05, **p < 0.01, ***p < 0.001, ****p < 0.0001. Bar = 75μm.

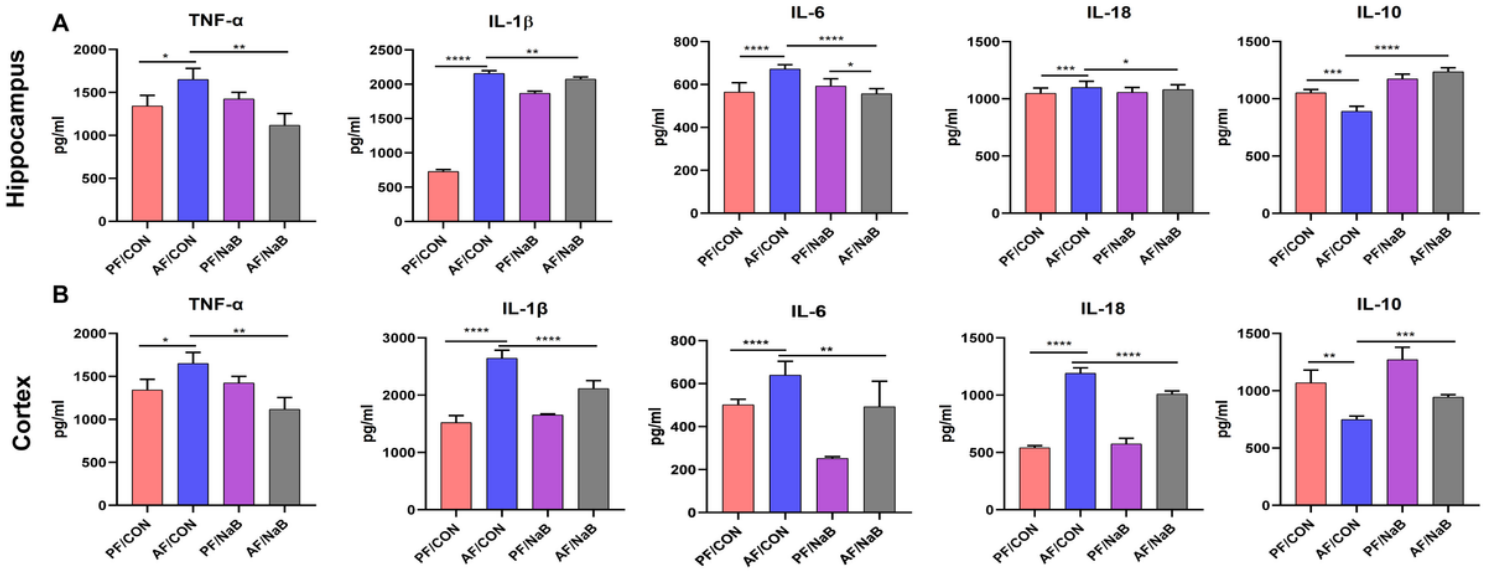

Figure 8

Sodium butyrate downregulated pro-inflammatory cytokines and upregulated anti-inflammatory factors expression in chronic alcohol exposed mice. (A) The concentrations of pro-inflammatory TNF-α, IL-6, IL-1β and IL-18 and anti-inflammatory IL-10 in the hippocampus; (B) The levels of TNF-α, IL-6, IL-1β, IL-18 as well as IL-10 in the prefrontal *cortex*. *$p < 0.05$, **$p < 0.01$, ***$p < 0.001$, ****$p < 0.0001$.

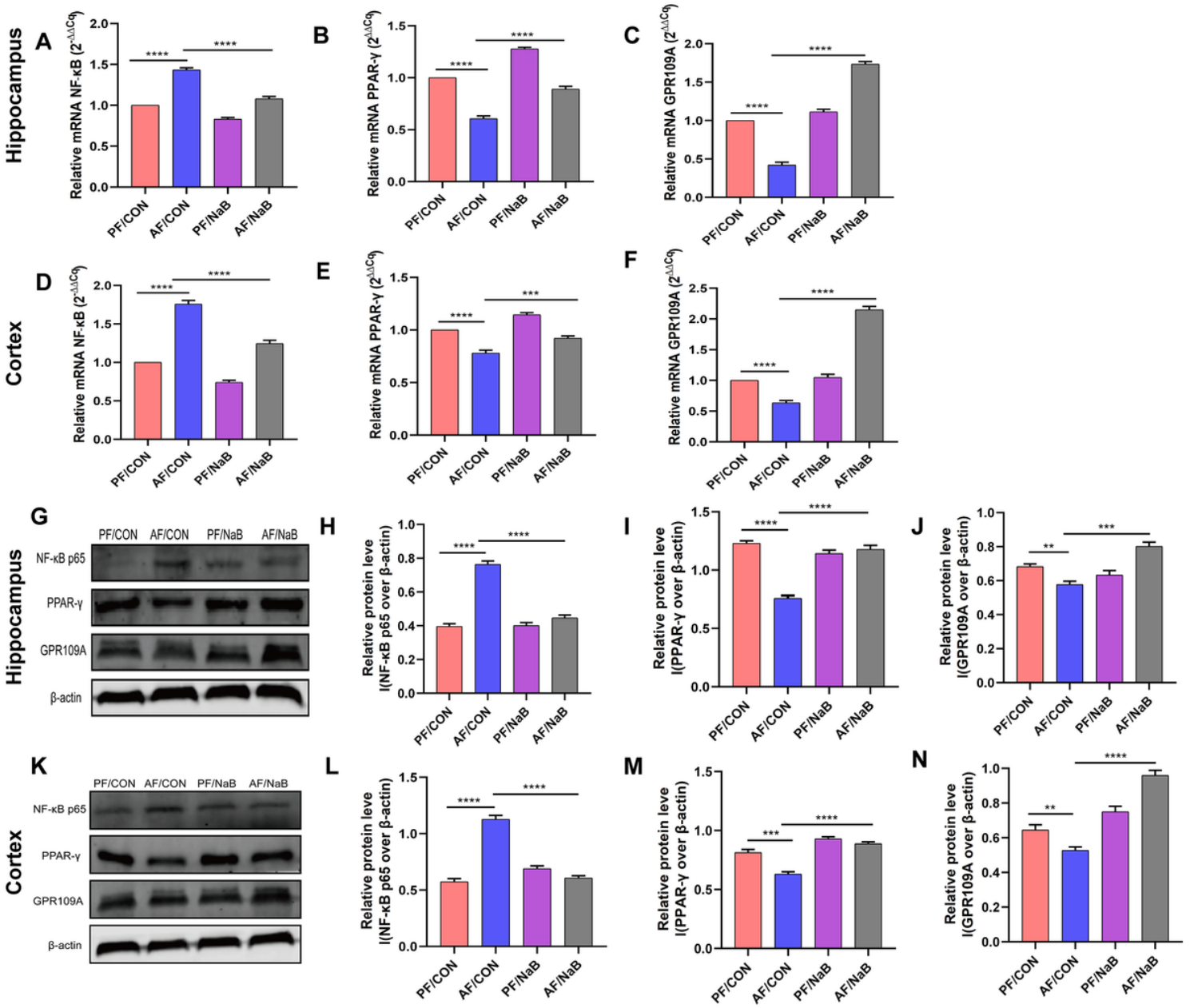

Figure 9

Sodium butyrate may attenuate neuroinflammation in the chronic alcohol exposed mice by regulating GPR109A receptor in microglia, increasing PPAR-γ, and inhibiting NF-κB expression. The mRNA levels of NF-κB p65 (A), PPAR-γ (B), GPR109A (C) in the hippocampus, and in the prefrontal cortex (D, E, F); (G) Representative western blot images and statistical results of NF-κB p65, PPAR-γ and GPR109A expressions of protein levels in the hippocampal tissues (H-J) and the expressions (K) in the cortical tissues (L-N), n=3, *$p < 0.05$, **$p < 0.01$, ***$p < 0.001$, ****$p < 0.0001$.

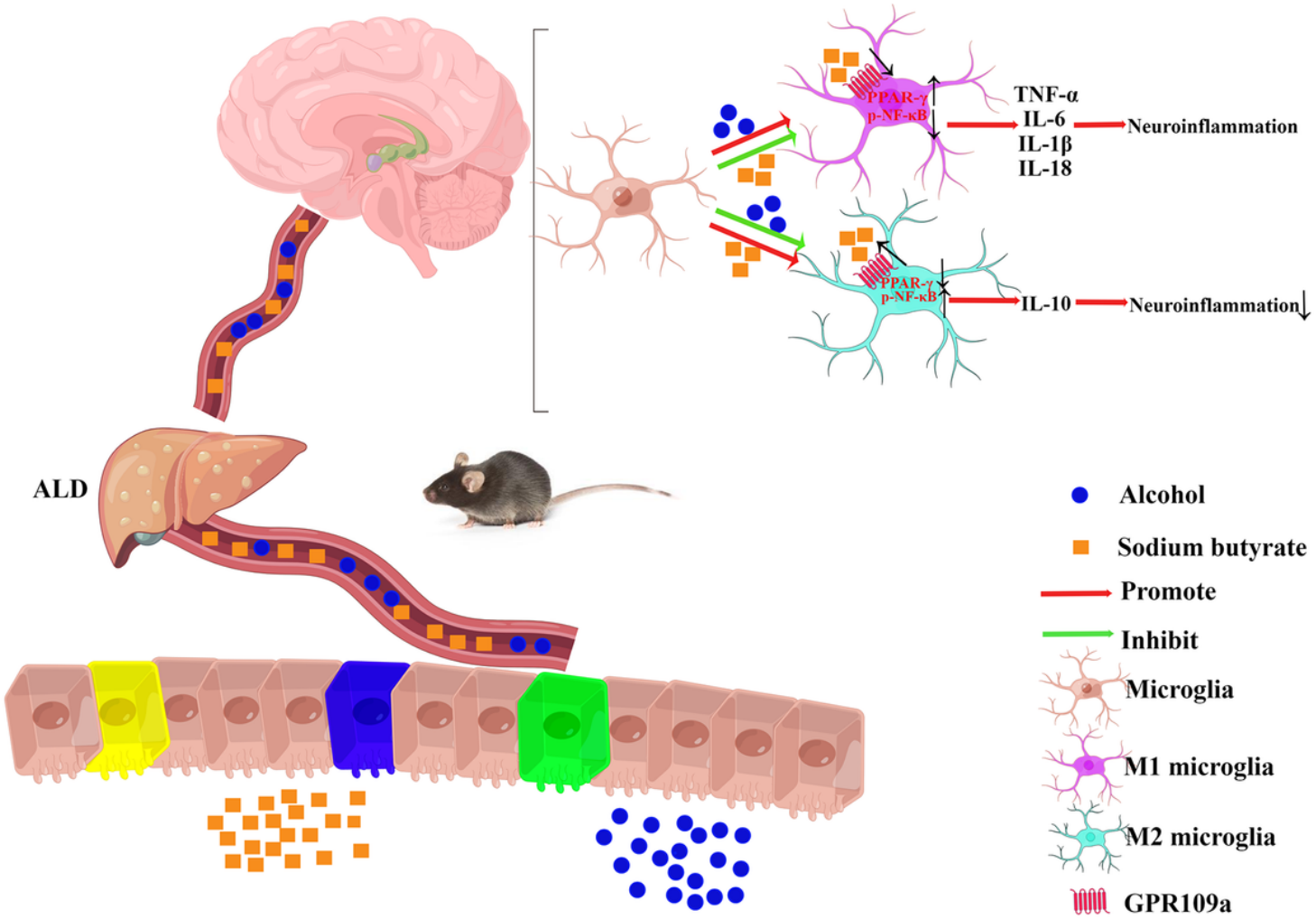

Figure 10

Sodium butyrate ameliorated alcohol-induced nerve damage by suppressing neuroinflammation through modulating microglia polarization in dependence on GPR109A/PPAR-γ/NF-κB pathway.

Supplementary Files

This is a list of supplementary files associated with this preprint. Click to download.

- FigureS1andS2.doc
- FigureS1.tif
- FigureS2.tif
- TableS1.docx